Int J Clin Exp Med 2018;11(2):603-611
www.ijcem.com /ISSN:1940-5901/IJCEM0046069

Original Article

Effects of valsartan on monocrotaline-induced right ventricular-pulmonary arterial uncoupling

Bin Wu[1*], Tao You[2*], Hongjia Zhao[3], Quehui Guo[2], Yanping Lian[2], Qiufang Ouyang[2]

[1]Department of Rehabilitation, Second Affiliated People's Hospital of Fujian Traditional Chinese Medicine University, Fuzhou, Fujian, China; [2]Department of Ultrasonography, Second Affiliated People's Hospital of Fujian Traditional Chinese Medicine University, Fuzhou, Fujian, China; [3]Department of Cardiology, Second Affiliated People's Hospital of Fujian Traditional Chinese Medicine University, Fuzhou, Fujian, China. [*]Equal contributors.

Received October 1, 2016; Accepted November 5, 2017; Epub February 15, 2018; Published February 28, 2018

Abstract: Objective: To investigate whether valsartan ameliorated monocrotaline (MCT)-induced right ventricular-pulmonary arterial (PA) uncoupling in rats and its possible mechanisms. Methods: Ninety Sprague-Dawley rats were divided randomly into control, MCT+vehicle, and MCT+valsartan groups. Right ventricle (RV) hemodynamic parameters were determined by echocardiography and invasive right ventricular cannulation. The morphological changes of RV and pulmonary arterioles were assessed. The interstitial fibrosis of RV myocardium and pulmonary was analyzed with Masson's trichrome staining. And RV myocardial apoptosis was detected by TUNEL assay. The protein expression of Fas, Bax, Bcl-2 and caspase-3 in RV myocardium was analyzed by Western Blotting. Results: RV-PA uncoupling, pulmonary vascular remodeling, RV hypertrophy, and interstitial fibrosis of lung and RV developed 3 wks after MCT administration. Alternatively, MCT induced RV apoptosis, associated with the upregulation of Fas, Bax, and caspase-3 expression, while downregulation of Bcl-2 expression. And these manifestations were significantly reversed by valsartan treatment. Conclusion: Valsartan can ameliorate RV-PA uncoupling, at least in part, by improving pulmonary arterioles and RV remodeling, and reducing collagen deposition, as well as lessening RV apoptosis via regulating the expression of Fas, caspase-3, Bcl-2 and Bax molecules in RV myocardium.

Keywords: Pulmonary hypertension, right ventricular dysfunction, monocrotaline, valsartan

Introduction

Pulmonary hypertension (PAH) is characterized by an increase in pulmonary vascular resistance as a consequence of pulmonary vascular remodeling. However, when the increased afterload cannot be compensated by ventricular contractility, ventricular-arterial uncoupling follows. And eventually right ventricle (RV) failure occurs [1, 2].

Monocrotaline (MCT)-treated rats model is widely applied for the study on the functional, structural, and molecular changes associated with PAH, RV compensated hypertrophy and RV failure [3, 4]. Mounting evidence suggests MCT induces PAH, promote cardiac interstitial fibrosis and RV failure [5]. However, little data is available on the effects of MCT on RV-pulmonary arterial uncoupling [6].

Apoptosis is regulated via the extrinsic pathway (death receptor-dependent pathway) and intrinsic pathway (mitochondria-dependent pathway). The ligation of death receptors and their ligands induces the formation of a death-inducing signaling complex, followed by the caspase-8 activation. Activated caspase-8 can transmit the apoptotic signals both in directly via caspase-3 activation and in indirectly via activation of pro-apoptotic B-cell lymphoma 2 (Bcl-2) family proteins. Activation of pro-apoptotic Bcl-2 family proteins can induce the mitochondrial permeabilization, resulting in the release of cytochrome c into the cytosol. In the intrinsic pathway, released cytochrome c can activate caspase-9, and then activated caspase-9 induces the cleavage of procaspase-3. Cleaved caspase-3 through the extrinsic and intrinsic pathways can interact with its substrates, resulting in cell death. It is reported

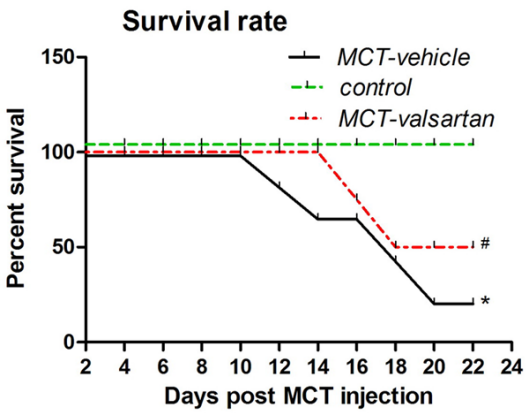

Figure 1. Survival curves of rats treated with valsartan. Survival rates were monitored during the treatment period from day 0 to 22. MCT: monocrotaline. $^{*}P<0.05$ *vs* normal control rats, $^{\#}P<0.05$ vs MCT model rats.

apoptosis plays an important role in the pathogenesis of RV remodeling. However, whether the molecules of Fas, caspase-3, Bcl-2 and Bax are closely associated with RV apoptosis is not yet fully understood. This study was to investigate whether those molecules were involved in RV apoptosis induced by MCT.

It is well recognized that valsartan can improve the survival rate [7] and inhibit apoptosis [8] in the monocrotaline (MCT)-injured rats. However, the roles of valsartan on RV-pulmonary arterial uncoupling and the underlying mechanism are not investigated as yet. Therefore, we explored the biological role of valsartan on RV-pulmonary arterial coupling and further investigated the potential underlying molecular mechanism.

Materials and methods

Animals and experimental protocol

All of the procedures and protocols were approved by Institutional Animal Care and Use Committee, Fujian University of Traditional Chinese Medicine and followed the guidelines issued by the National Institutes of Health Guide for the Care and Use of Laboratory Animals. Ninety adult male Sprague-Dawley (SD) rats were divided randomly into the control group, MCT+vehicle group, and MCT+valsartan group (n=30 for each group, 10 rats were used for survival analysis, and the remaining 20 rats were used for morphological and haemodynamic studies). On the first day, MCT+vehicle rats and MCT+valsartan rats were administered with MCT (50 mg/kg, Sigma-Aldrich, Louis, MO, USA) by subcutaneous injection, while the control rats were injected with same dose of saline. The MCT+vehicle rats were intragastrically (i.g.) administered with valsartan (20 mg/kg·d) for 21 days, while the control and MCT+vehicle rats were given the same dose of saline.

Echocardiography

B-mode, M-mode and pulmonary pulsed-wave Doppler echocardiography (Philips, Eindhoven, Netherlands) was serially performed to monitor the stage of disease. The parameters of ejection fraction in left ventricle and RV were determined. And the tricuspid annular plane systolic excursion (TAPSE, an index of the RV systolic function) was measured as the fractional shortening in M-mode, between the apex and the lateral tricuspid annulus in the apical four chamber view. Echocardiography was performed and analyzed by the investigators (O.Y. Q.F. and X.R., with 8 and 7 years of experience in echocardiography, respectively) in a blind fashion.

Right ventricular hemodynamics

All surviving rats underwent haemodynamic measurement on the 22nd day after MCT injection. Rats were anesthetized with a combination of 80 mg/kg ketamine and 5 mg/kg acepromazine (both form Sigma-Aldrich, St. Louis, MO, USA). After opening of the thorax, a temporal ligature was placed around the inferior vena cava. Following an apical stab (23 G), a combined pressure-volume catheter (SPR-869, Millipore, Billerica, MA, USA) was introduced to the RV and positioned along its long axis. RV peak systolic pressure (RVSP), RV end-diastolic pressure, and RV end-systolic pressure, RV contraction and relaxation rates ($RVdp/dt_{max}$ and $RV dp/dt_{min}$) were assessed. Effective pulmonary arterial elastance (Ea), as a measurement of RV afterload, was calculated as end-systolic pressure divided by stroke volume. Meanwhile, Ees, an indicator of ventricle end-systolic elastance, was determined. Ea/Ees was determined as an indicator of ventricular-arterial coupling.

Morphometric analysis right ventricular hypertrophy and pulmonary remodeling

For pulmonary morphometry, lung paraffin sections (4 μm) were stained with hematoxylin and eosin (HE) staining and examined using light microscopy (Olympus, Center Valley, PA, USA).

Table 1. Hemodynamic parameters determined by echocardiography and cannulation ($\bar{x} \pm s$)

	Control	MCT-vehicle	MCT-valsartan
RV-EF, %	45.349 ± 4.417	37.425 ± 8.549*	41.528 ± 5.451
LV-EF, %	63.587 ± 7.514	61.428 ± 10.372	64.525 ± 12.66
HR, beats/min	349.451 ± 55.63	335.46 ± 68.121	361.58 ± 55.425
RVSP, mmHg	26.549 ± 4.697	48.327 ± 10.874*	40.641 ± 8.752#
TAPSE, mm	1.798 ± 0.311	1.182 ± 0.251*	1.583 ± 0.247#
dP/dt_{max}, mmHg/s	2589.425 ± 248.216	1801.268 ± 408.294*	2015.752 ± 258.149#
dP/dt_{min}, mmHg/s	-1376.504 ± 100.207	-1673.251 ± 298.587*	-1341.282 ± 150.457#
RV-Pes, mmHg	20.601 ± 4.059	47.015 ± 12.534	30.948 ± 9.127#
RV-Ea, mmHg/μl	0.176 ± 0.087	0.258 ± 0.067*	0.236 ± 0.109#
RV-Ees, mmHg/μl	0.104 ± 0.026	0.094 ± 0.029	0.114 ± 0.045#
RV-Ea/Ees	1.694	2.745	2.097#

MCT: monocrotaline; RV: right ventricle; LV: left ventricle; EF: ejection fraction; HR: heart rate; RVSP: RV systolic pressure; Pes: end-systolic pressure; TAPSE: tricuspid annular plane systolic excursion; dP/dt_{max}: maximal rate of pressure increase; dP/dt_{min}: maximal rate of pressure decline; Ea: effective arterial elastance; Ees: end-systolic elastance. *P<0.05 *vs* normal control rats, #P<0.05 vs MCT model rats. Results were expressed as mean ± SE for 20 rats in each group.

Averages of at least 20 vessels from each animal were measured from each rat. The percent wall thickness was calculated using the following formula: wall thickness (%) = [medial thickness ×2/external diameter] ×100. And wall area (%) = [($area_{ext}$-$area_{int}$)/$area_{ext}$] ×100.

For myocardial histopathology, the hearts were isolated, flushed with saline, the gross specimens were photographed to analyze the RV free wall thickness. Subsequently, the right ventricle was separated from the left ventricle septum (LV_S). The ratio of RV weight to the weight of left ventricle plus septum (LV+S) was calculated for each heart and was used as an index of RV hypertrophy.

Masson's trichrome staining for pulmonary and RV myocardial interstitial fibrosis

Masson's trichrome staining (Masson's trichrome kit, Sigma-Aldrich, St. Louis, MO, USA.) was performed for lung and myocardial interstitial fibrosis. The percentage area of fibrosis for each specimen was calculated.

TUNEL assay

In situ terminal deoxynucleotidyl-transferase-mediated dUTP nick-end labeling (TUNEL) assay was performed on sections of RV myocardium using a commercially available kit (In Situ Cell Death Detection Kit; Roche, Basel, Switzerland) according to the manufacturer's instructions. The number of TUNEL-positive cardiomyocyte nuclei was expressed as percentage of the total number of cardiomyocyte nuclei and called the apoptosis index.

Western blot analysis for Fas, Bax, Bcl-2, Caspase-3 in right ventricular myocardium

Western blot analysis was performed to determine the Fas, Bax, Bcl-2, Caspase-3 expression in right ventricular myocardium. Proteins (30 μg) were run on a 10% SDS-PAGE gel and transferred to polyvinylidene fluoride membranes. Following incubation with 10% non-fat milk for 1 h, the membranes were probed with primary antibody (Fas, Bax, Bcl-2, and Caspase-3 all diluted at 1:500, Abcam, Cambridge, UK) overnight at 4°C and then incubated with HRP-labeled goat anti-mouse secondary antibodies (1:2,000; Santa Cruz Biotechnology, Inc., Dallas, TX, USA). The protein levels were normalized using β-actin as a loading control. The relative optical density of the protein bands was measured using a Zeineh Laser Densitometer (Biomed Instruments, Inc., Fullerton, CA, USA) after subtracting the film background.

Statistical analysis

All the values were expressed as the mean ± standard error (SE) unless otherwise indicated. The group comparisons were performed with the analysis of variance. The Mann-Whitney U test was used if the variance was not normally distributed. A *P*-value of 0.05 was accepted as

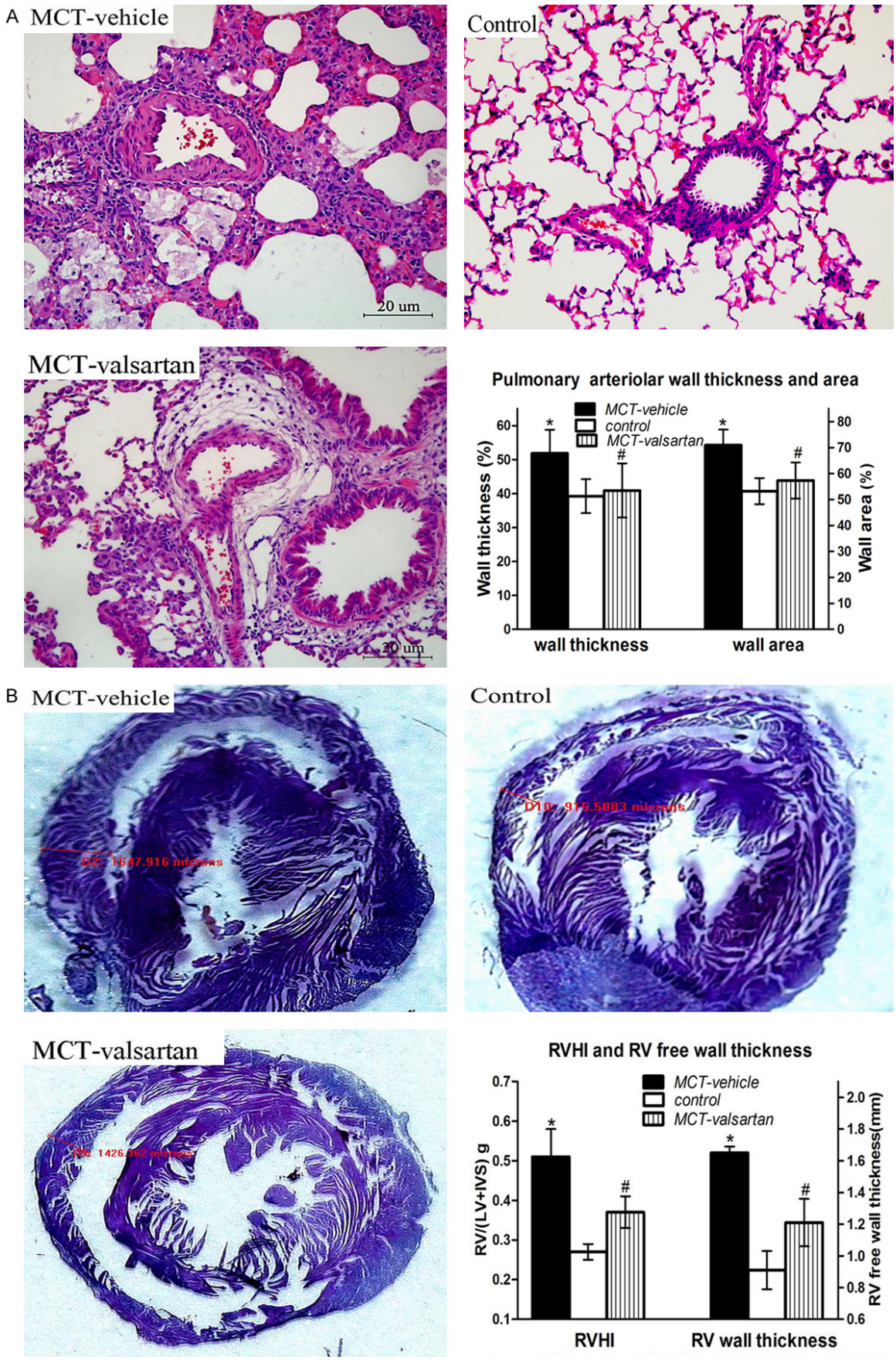
A
MCT-vehicle
20 um
Control
MCT-valsartan
20 um
Pulmonary arteriolar wall thickness and area
MCT-vehicle
control
MCT-valsartan
Wall thickness (%)
Wall area (%)
wall thickness
wall area
B
MCT-vehicle
Control
MCT-valsartan
RVHI and RV free wall thickness
MCT-vehicle
control
MCT-valsartan
RV/(LV+IVS) g
RV free wall thickness(mm)
RVHI
RV wall thickness

Figure 2. Valsartan attenuated pulmonary vascular remodeling and right ventricle hypertrophy in MCT-injured rats. MCT-vehicle animals exhibited a significant increase in wall thickness of pulmonary arterioles (A) and right ventricle myocardium (B), which was inhibited by valsartan treatment. RVHI: right ventricle hypertrophy index; MCT: monocrotaline. Histogram represented mean ± SE of 20 rats. $^{*}P<0.05$ *vs* normal control rats, $^{\#}P<0.05$ vs MCT model rats.

significant. The statistical analysis was performed using SPSS 17.0 software.

Results

Effects of valsartan on mortality

Survival rate of the MCT-vehicle rats decreased gradually to 31.5% on the 22nd day (P<0.05 versus control). All animals in MCT-vehicle group manifested weight loss, ruffled fur, hunched posture, lethargy, dyspnea and labored breathing involving abdominal accessory muscles since the 11th day post MCT injection. While none of the control vehicle-treated rats died during the same period. Treatment with valsartan markedly improved the survival rate (**Figure 1**). Autopsies revealed that the major causes of death in MCT-vehicle rats were cardiopulmonary abnormity.

Right ventricular hemodynamics

Echocardiography was performed every 3 days during the period of observation. The RV EF was significantly lower on the 22nd day after MCT injection than age-matched normal controls, which was reversed by valsartan treatment (**Table 1**). Alternatively, TAPSE in MCT-vehicle rats decreased significantly relative to normal control animals, which was improved by valsartan treatment. The LV ejection fraction was not altered in MCT-vehicle rats, although it increased marginally in valsartan-treated rats.

Additionally, RV systolic pressure (RVSP) and Pes were notably higher in MCT-vehicle rats than in control animals. RV contractility (determined by dp/dt_{max}) and RV relaxation (indicated by dp/dt_{min}) were attenuated in MCT-vehicle rats. Valsartan treatment caused a significant reduction in RV systolic pressure and Pes, but an increase in dp/dt_{max} and dp/dt_{min}, as compared with those in MCT-vehicle group.

As for Ea/Ees, it averaged 1.694 in normal control, suggesting ventricular-arterial coupling matched well. Conversely, rats exposure to MCT for 21 days exhibited ventricular-arterial uncoupling, as evidenced by the increased Ea/Ees, owing to a disproportionate increase in Ea while a marginal reduction in Ees. Strikingly, valsartan partly restored ventricular-arterial coupling, as evidenced by reduced RV afterload and preserved RV systolic function.

Pulmonary arterioles remodeling and RV hypertrophy

The wall thickness and area of pulmonary arterioles were significantly increased in MCT-vehicle rats compared to controls (52.31 ± 4.14% vs 38.42 ± 5.09%, 76.78 ± 8.92% vs 50.13 ± 6.04%, both *P*<0.05). Treatment with valsartan reduced significantly the wall thickness (42.76 ± 2.87%) and wall area (59.27 ± 3.36%). Simultaneously, MCT administration substantially increased the weight ratio of RV to left ventricle plus septum (RVHI) and the RV free wall thickness as compared with control rats. Valsartan treatment delayed the progression of RV hypertrophy, as manifested by attenuated RVHI and free wall thickness. Collectively, these data indicated that valsartan inhibited pulmonary arterioles remodeling and RV hypertrophy induced by MCT (**Figure 2**).

Valsartan treatment alleviated interstitial fibrosis induced by MCT

Cardiopulmonary interstitial fibrosis was semiquantified according to Masson's trichrome staining (**Figure 3**). MCT injection caused a strong fibrotic response on the 22nd day relative to normal control rats (18.2 ± 2.7% vs 4.6 ± 0.5%), which was substantially inhibited by valsartan treatment (9.4 ± 1.3%). In RV myocardium, the fibrosis was significantly higher in MCT-vehicle group than that in normal control group. However, the extent of fibrosis did not differ significantly between the MCT-vehicle and MCT-valsartan groups.

Valsartan reversed RV apoptosis induced by MCT

In normal control rats, the myocardial nuclei were stained green (normal nuclei), no brownish yellow nuclei (apoptotic nuclei) were observed (**Figure 4**). The percentage of apoptotic cells, however, was dramatically increased in

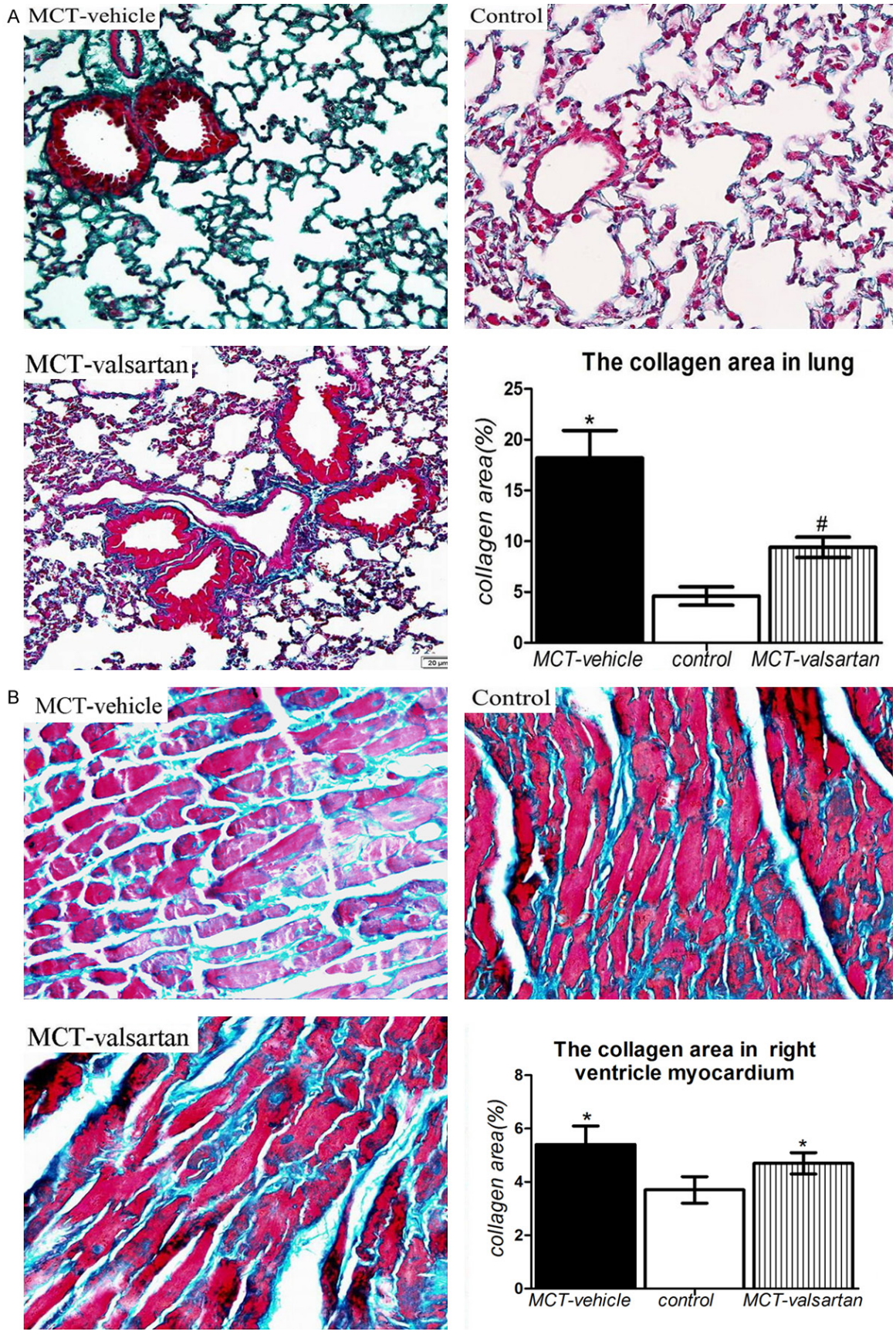
A
MCT-vehicle
Control
MCT-valsartan
The collagen area in lung
collagen area(%)
25
20
15
10
5
0
*
#
MCT-vehicle
control
MCT-valsartan
B
MCT-vehicle
Control
MCT-valsartan
The collagen area in right ventricle myocardium
collagen area(%)
8
6
4
2
0
*
*
MCT-vehicle
control
MCT-valsartan

Figure 3. Lung and right ventricle myocardial interstitial fibrosis as illustrated by masson's trichrome staining. Fibrosis appeared as green fibers, whereas cytoplasm was stained red (400×). MCT-vehicle animals displayed substantially increased fibrosis in lung (A) and in right ventricle myocardium (B), which was ameliorated by valsartan treatment. Results were expressed as mean ± SE for 20 animals in each group. MCT: monocrotaline. $^{*}P<0.05$ *vs* normal control rats, $^{\#}P<0.05$ vs MCT model rats.

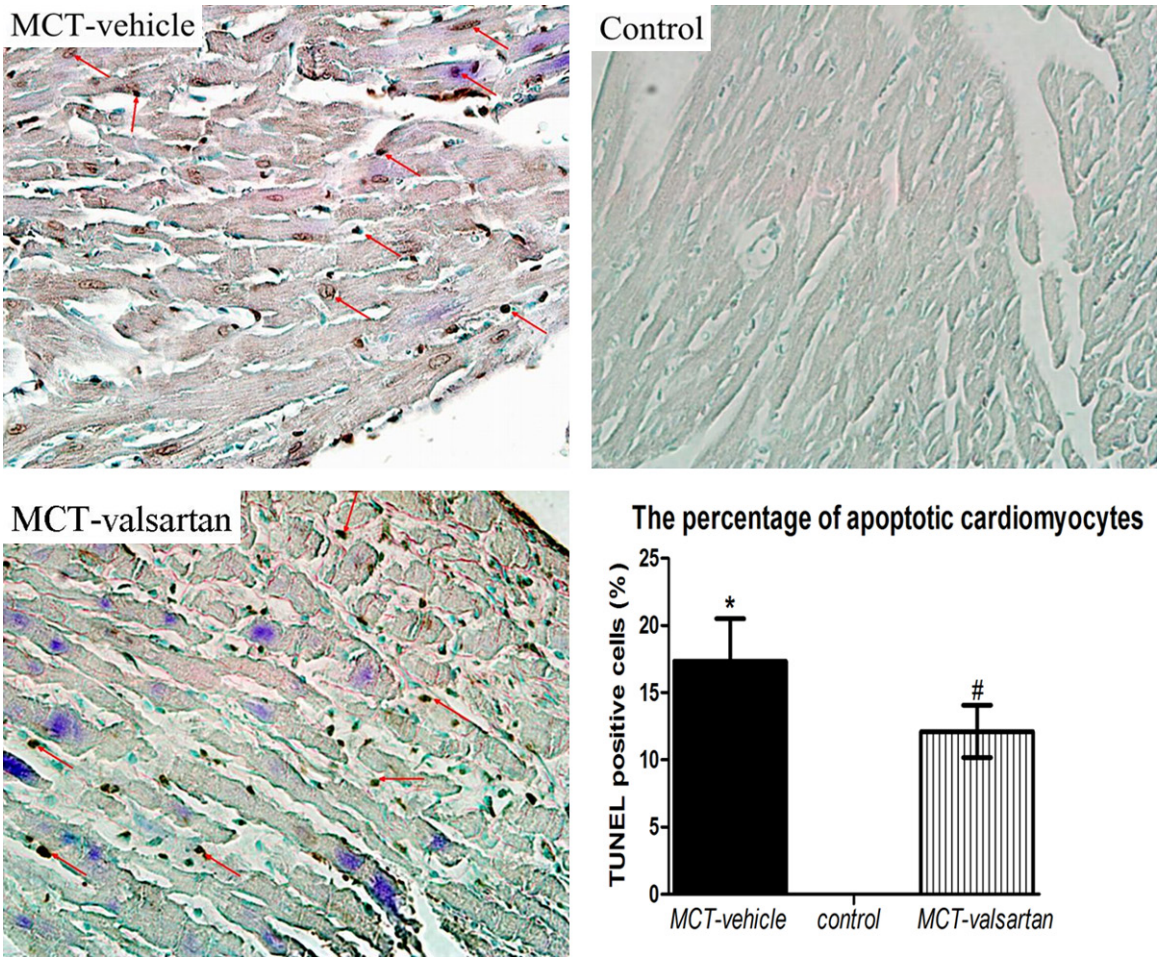

Figure 4. Effects of valsartan on myocardial apoptosis as depicted by TUNEL assay (original magnification ×400). Brownish yellow nuclei indicated apoptotic nuclei (arrow). MCT induced RV apoptosis, which was ameliorated by valsartan treatment. Histogram represented mean ± SE for 20 animals in each group. MCT: monocrotaline. $^{*}P<0.05$ *vs* normal control rats, $^{\#}P<0.05$ vs MCT model rats.

the MCT-vehicle rats (18.35 ± 2.56%), which was *reversed* by valsartan treatment.

Effects of valsartan on the expression of Fas, caspase-3, Bcl-2 and Bax expression in right ventricle myocardium

Compared with the normal control group, the expression of Fas, Bax, and caspase-3 was increased, while the expression of Bcl-2 was decreased in MCT-vehicle group (**Figure 5**). Valsartan treatment could partially reduce the expression of Caspase-3, Bax, and Fas, while enhance the expression of Bcl-2.

Discussion

In this study, we successfully established a RV-pulmonary arterial uncoupling rats model by a single subcutaneous injection of MCT. These rats displayed pulmonary vascular remodeling, RV hypertrophy, cardiopulmonary interstitial fibrosis, and RV apoptosis, which were consistent with previous studies [9, 10]. We also demonstrated for the first time that valsartan effectively ameliorated RV-pulmonary arterial structural remodeling and functional coupling, as well as RV apoptosis via the expression of Fas, caspase-3, Bcl-2 and Bax.

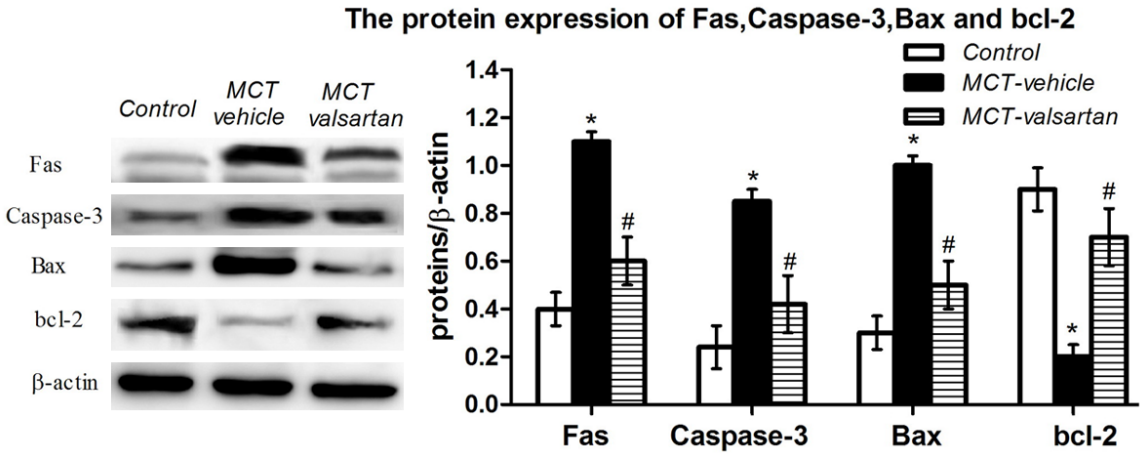

Figure 5. Effects of valsartan on the expression of Fas, caspase-3, Bcl-2 and Bax expression in right ventricle myocardium as manifested by western blotting. Valsartan reduced the expression of Caspase-3, Bax and Fas, while enhanced the expression of Bcl-2 in right ventricle myocardium of MCT-injured rats. Histogram represented mean ± SE for 20 animals in each group. MCT: monocrotaline. $^{*}P<0.05$ *vs* normal control rats, $^{\#}P<0.05$ *vs* MCT model rats.

The arterial system works in combination with the heart to deliver blood to the lung or peripheral tissues. Ea/Ees, describes the coupling between the ventricular and arterial systems. The normal operating range of Ea/Ees occurs when the coupled system works with the maximal efficiency. Our data illustrated the ratio of Ea/Ees was 1.694 in normal control rats, well within the range of optimal function. While in MCT-injured rats, the ratio increased (2.745). And those results were substantiated by the investigators who reported MCT-injected animals exhibited right ventricular-arterial uncoupling [11]. We demonstrate firstly that valsartan can ameliorate ventricular-arterial coupling (2.097) by decreased Ea, and by marginally increased Ees.

Our results indicated that RV fibrosis was higher in MCT-vehicle and control rats. This is in agreement with the findings that MCT can induce RV fibrosis [12]. However, this result was somewhat at odds with the report that RV interstitial fibrosis remained comparable between MCT-treated rats and normal controls [13]. The inconsistency may be explained by the difference in the MCT dose and the period of disease progression.

Individual damage would trigger DNA damage response through distinct yet overlapping pathways to regulate apoptosis. The Bcl-2 family includes Bax and Bcl-2, which are involved in the mitochondrial apoptotic pathway and the Bcl-2/Bax ratio determines cell apoptotic fate [14]. The ligation of Fas by the up-regulated FasL promotes their clustering to form a complex. This action, recruits the adaptor protein Fas-associated protein with death domain (FADD) through death domain and interactions with proteins such as procaspase-8, following the activation of caspase-3, leading to cell death. The activation of caspase-3 is often considered as the point-of-no-return in the apoptotic signaling. Our results suggested that valsartan improved RV apoptosis induced by MCT, with a concomitant decrease in Fas, Caspase-3, and Bax/Bcl-2 ratio. This anti-apoptotic effect may, at least in part, relate to the regulation of Fas, Caspase-3, and Bax/Bcl-2.

In conclusion, our data illustrated valsartan could ameliorate right ventricular-pulmonary arterial uncoupling induced by MCT in rats. The mechanism may be associated with reduced pulmonary arterioles and RV remodeling, attenuated lung fibrosis, and alleviated RV apoptosis via the molecules of Fas, caspase-3, Bcl-2 and Bax. Based on these findings, valsartan might be a novel alternative medicine for the treatment of PAH. There are, however, several caveats regarding this study. Given the animal model is not fully representative of the human disease, and therefore the results observed must be interpreted with caution. Additionally, due to the complexity in the pathogenesis of right ventricular-pulmonary arterial uncoupling, the roles of other neurohumoral factors, calcium channel in our model thus warrant further investigation.

Acknowledgements

This work was supported by Natural Science Foundation of Fujian Province (2013J01321), Key Cooperative Project on University Industry-Education by Fujian Science and Technology Commission (2011Y4004).

Disclosure of conflict of interest

None.

Address correspondence to: Qiufang Ouyang, Department of Ultrasound, Second Affiliated People's Hospital, Fujian University of Traditional Chinese Medicine, 282 Wusi Road, Gulou District, Fuzhou, Fujian, China. Tel: +86-0591-87878122; Fax: +86-0591-87878125; E-mail: 2602271822@qq.com

References

[1] Yang DL, Zhang HG, Xu YL, Gao YH, Yang XJ, Hao XQ, Su M, Wang XQ and Li XH. Galphaq-protein carboxyl terminus imitation polypeptide (GCIP)-27 inhibits right ventricular hypertrophy induced by monocrotaline in rats. Biol Pharm Bull 2009; 32: 376-381.

[2] Ghuysen A, Lambermont B, Kolh P, Tchana-Sato V, Magis D, Gerard P, Mommens V, Janssen N, Desaive T and D'Orio V. Alteration of right ventricular-pulmonary vascular coupling in a porcine model of progressive pressure overloading. Shock 2008; 29: 197-204.

[3] Ishiguro-Oonuma T, Suemoto M, Okada M, Yoshioka K, Hara Y, Hashizume K and Kizaki K. Aberrant gene expression of heparanase in ventricular hypertrophy induced by monocrotaline in rats. J Vet Med Sci 2016; 78: 499-503.

[4] Yoshiyuki R, Fukushima R, Tanaka R and Machida N. Comparison of preventive effect of sildenafil and therapeutic effect of sildenafil treatment in rats with monocrotaline-induced pulmonary arterial hypertension. J Vet Med Sci 2016; 78: 1607-1610.

[5] Guihaire J, Haddad F, Boulate D, Decante B, Denault AY, Wu J, Hervé P, Humbert M, Dartevelle P, Verhoye JP, Mercier O and Fadel E. Non-invasive indices of right ventricular function are markers of ventricular-arterial coupling rather than ventricular contractility: insights from a porcine model of chronic pressure overload. Eur Heart J Cardiovasc Imaging 2013; 14: 1140-1149.

[6] Kass DJ, Rattigan E, Kahloon R, Loh K, Yu L, Savir A, Markowski M, Saqi A, Rajkumar R, Ahmad F and Champion HC. Early treatment with fumagillin, an inhibitor of methionine aminopeptidase-2, prevents pulmonary hypertension in monocrotaline-injured rats. PLoS One 2012; 7: e35388.

[7] Usui S, Yao A, Hatano M, Kohmoto O, Takahashi T, Nagai R, Kinugawa K. Upregulated neurohumoral factors are associated with left ventricular remodeling and poor prognosis in rats with monocrotaline-induced pulmonary arterial hypertension. Circ J 2006; 70: 1208-1215.

[8] Campian ME, Verberne HJ, Hardziyenka M, de Bruin K, Selwaness M, van den Hoff MJ, Ruijter JM, van Eck-Smit BL, de Bakker JM, Tan HL. Serial noninvasive assessment of apoptosis during right ventricular disease progression in rats. J Nucl Med 2009; 50: 1371-1377.

[9] Okada M, Harada T, Kikuzuki R, Yamawaki H, Hara Y. Effects of telmisartan on right ventricular remodeling induced by monocrotaline in rats. J Pharmacol Sci 2009; 111: 193-200.

[10] Zuo XR, Wang Q, Cao Q, Yu YZ, Wang H, Bi LQ, Xie WP, Wang H. Nicorandil prevents right ventricular remodeling by inhibiting apoptosis and lowering pressure overload in rats with pulmonary arterial hypertension. PLoS One 2012; 7: e44485.

[11] de Man FS, Handoko ML, van Ballegoij JJ, Schalij I, Bogaards SJ, Postmus PE, van der Velden J Westerhof N Paulus WJ and Vonk-Noordegraaf A. Bisoprolol delays progression towards right heart failure in experimental pulmonary hypertension. Circ Heart Fail 2012; 5: 97-105.

[12] Lourenço AP, Roncon-Albuquerque R Jr, Brás-Silva C, Faria B, Wieland J, Henriques-Coelho T, Correia-Pinto J and Leite-Moreira AF. Myocardial dysfunction and neurohumoral activation without remodeling in left ventricle of monocrotaline-induced pulmonary hypertensive rats. Am J Physiol Heart Circ Physiol 2006; 291: H1587-94.

[13] Hessel MH, Steendijk P, den Adel B, Schutte CI and van der Laarse A. Characterization of right ventricular function after monocrotaline-induced pulmonary hypertension in the intact rat. Am J Physiol Heart Circ Physiol 2006; 291: H2424-30.

[14] Piao L, Marsboom G, Archer SL. Mitochondrial metabolic adaptation in right ventricular hypertrophy and failure. J Mol Med 2010; 88: 1011-1020.